Manipulation of cold atoms using a corrugated magnetic reflector

Article (Published Version)

PHYSICAL REVIEW A, VOLUME 61, 031404(R)

Manipulation of cold atoms using a corrugated magnetic reflector

P. Rosenbusch, B. V. Hall, I. G. Hughes,* C. V. Saba, and E. A. Hinds†
Sussex Centre for Optical and Atomic Physics, University of Sussex, Brighton, BN1 9QH, United Kingdom
(Received 20 September 1999; published 11 February 2000)

A corrugated magnetic reflector is realized by adding a bias field to a static magnetic mirror. This permits real-time manipulation of a cold-atom cloud on time scales down to 100 μs. We show that rotation of the bias field generates a traveling corrugation of adjustable depth and velocity. Momentum is transferred from the traveling wave to the atoms, resulting in a displacement of the cloud that depends on the wave velocity. This is a step towards a new method of manipulation in which neutral atoms could be transported across the surface by surfing along the moving wave.

PACS number(s): 32.80.Pj, 03.75.Be, 39.10.+j

The last few years have seen intense interest in manipulating laser-cooled atoms by various mirrors, lenses, and gratings. Much effort has been devoted to optical methods reviewed in Ref. [1], but great progress has recently been made using static magnetic fields as reviewed in Ref. [2]. For example, atom clouds and beams have been controlled by microscopically patterned magnetic surfaces [3] and millimeter-sized arrays of magnets [4]. Such devices do not heat the atoms and they can have a large active area. Until recently, however, they could not be modulated and were therefore unsuitable for time-dependent atom optics [5]. Microfabricated arrays of current-carrying wires have provided one powerful approach to achieving time-dependent magnetic fields [6]. In this Rapid Communication we demonstrate another method. We show that a bias field added to a microstructured permanent-magnet mirror produces a static, oscillating, or traveling corrugation. We also show that momentum is transferred from the traveling wave to the atoms, resulting in a displacement of the cloud that depends on the wave velocity. This is a step towards a kind of ''conveyor belt'' or motor for atoms, which could move them across the surface [7]. Atom transport promises to be an important aspect of the rapidly developing field of integrated atom optics, in which cold atoms confined above a microfabricated surface are made to flow and interact with each other along prescribed paths in an analog of conventional integrated electronics [8,2,9].

Our reflector is a piece of videotape on which we have recorded a magnetization $M_0\cos(kx)\hat{\mathbf{x}}$, $\hat{\mathbf{x}}$ being a unit vector in the plane of the tape. The magnetostatic potential at height y above the surface decays as e^{-ky}, resulting [2] in a magnetic field of the form $B_1e^{-ky}[-\cos(kx)\hat{\mathbf{x}}+\sin(kx)\hat{\mathbf{y}}]$. The Zeeman energy of an atom above the surface is $U=-\mu_\zeta B_1e^{-ky}$, where μ_ζ is the projection of the magnetic moment onto the local magnetic field. For atoms moving sufficiently slowly, μ_ζ is a constant of the motion and the interaction potential depends only on the height y. The gradient of U gives a force perpendicular to the surface and repels the atom when μ_ζ is negative. This principle has been the basis of all the magnetic mirror experiments to date. Here we investigate the addition of a small uniform applied field (B_x,B_y,B_z), which does not perturb the magnetization of the surface appreciably but simply adds to the field of the mirror. This gives the adiabatic potential

$$U=-\mu_\zeta[B_1^2e^{-2ky}-2B_1B_G\cos(kx+\delta)e^{-ky}+B_G^2+B_z^2]^{1/2},$$

where $B_G^2=B_x^2+B_y^2$ and $\tan\delta=B_y/B_x$. In our experiments, $B_1\approx 667$ G is much greater than B_G and B_z, which are both $\lesssim 1$ G. The potential close to the surface is therefore that of the unperturbed mirror $-\mu_\zeta B_1e^{-ky}$ plus a corrugation or grating, $\mu_\zeta B_G\cos(kx+\delta)$. The possibility of producing a grating in this way was first pointed out by Opat *et al.* [10], but no experimental study of magnetic grating dynamics has been reported to date. In this Rapid Communication we first demonstrate the existence of the grating by measuring the angular distribution of atoms scattered from it and show that the blaze can be adjusted by altering the strength of B_G. We emphasize that in this experiment the pattern of reflected atoms is entirely classical and does not require the diffraction of de Broglie waves to be understood. Next, we investigate the interaction of atoms with a grating whose amplitude oscillates. Finally, we show, as was proposed in Ref. [7], that a rotating field generates a moving grating that can be used to transport atoms across the surface.

Before presenting the experiment, we develop a simple approximate theory that explains the main features we observe. We distinguish two regions of space. (i) Far from the reflector, $B_1e^{-ky}<B_G$, the force on the atom is weak and we neglect it. (ii) Close in, $B_1e^{-ky}>B_G$, and the force is

$$F_x\approx k\mu_\zeta B_G\sin(kx+\delta),\quad F_y\approx -k\mu_\zeta B_1e^{-ky}. \qquad (1)$$

This separates the x and y components of the motion. An atom dropped from height $y=h$ spends a total amount of time $T_{\rm int}$ in the inner region (ii) given by [2]

$$T_{\rm int}=\frac{4}{k\sqrt{2gh}}\,\mathrm{sech}^{-1}\left(\sqrt{\frac{-\mu_\zeta B_G}{mgh}}\right). \qquad (2)$$

Suppose also that the x coordinate of the atom does not change appreciably in the mirror field (Raman-Nath approximation [11]). The transverse momentum imparted by reflec-

*Present address: Department of Physics, University of Durham, South Road, Durham DH1 3LE, United Kingdom
†Electronic address: e.a.hinds@sussex.ac.uk

tion is then $F_x T_{\rm int}$, and the atom rises to its original height in a time $\sqrt{2h/g}$ with lateral displacement $\xi = \xi_0 \sin(kx+\delta)$, where

$$\xi_0 = \frac{4\mu_\zeta B_G}{mg} \operatorname{sech}^{-1}\left(\sqrt{\frac{-\mu_\zeta B_G}{mgh}} \right). \tag{3}$$

In a simpler model, the atoms reflect from the highest accessible equipotential as though from a hard surface, and then the sech^{-1} factor is absent. This is a poor approximation, however, as this factor lies between 2 and 4 for a wide range of experimental parameters.

Our apparatus collects $\sim 5\times 10^6$ ^{85}Rb atoms in a conventional magneto-optic trap (MOT), cools them to 24 μK in optical molasses, and optically pumps them into the $|F=3, m_F=+3\rangle$ ground state [1,3]. Now the cloud falls in the dark under gravity onto the concave reflector, which is magnetized with a wavelength $\lambda = 2\pi/k$ of 25.4 μm and has radius of curvature $R = 54$ mm [3]. After reflection, a pulse of laser light (5 ms, 60 μW/cm^2 σ^+ standing wave) produces enough fluorescence for a charge-coupled-device (CCD) camera to record the distribution of reflected atoms without appreciably moving them under radiation pressure.

The atoms are released from a height $h = R/2$ (i.e., 27.0 mm) so that the initial compact cloud is reconstructed 148 ms later at the original height after reflection from the smooth mirror. This is shown at the bottom of Fig. 1. The CCD image is on the left, with its (almost) Gaussian intensity profile plotted on the right. The width, 3.3 mm full width at half-maximum (FWHM) is virtually all due to the initial width of the cloud and determines the resolution of our subsequent experiments. The mirror is corrugated by adiabatically turning on B_G in the $\hat{\mathbf{y}}$ direction, 54 ms after the release of the cloud from molasses. The left side of Fig. 1 shows cloud images measured with various values of B_G, chosen to be multiples of 0.13 G. Each image has had background light subtracted by the following procedure. Atoms are collected as usual, but the molasses is tuned to resonance, causing rapid expansion of the cloud. After the usual 148-ms delay, the background image is taken and then subtracted pixel-by-pixel from the image where the cloud was not blown away. On the right of Fig. 1 we show the intensity profiles of every second image: the cloud first broadens then splits into a double-peaked structure as B_G increases. According to Eq. (3), a point cloud illuminating many wavelengths of the reflector should exhibit a final number distribution $dN/d\xi$ proportional to $1/\sqrt{\xi_0^2-\xi^2}$. After convolving this with the $B_G = 0$ instrumental distribution, we obtain profiles close to the experimental ones, indicating that our simple two-zone model is qualitatively correct. They are, however, 10 percent narrower than the experimental curves, so we also numerically integrated the equations of motion for a 24-μK point cloud. After convolution with the $B_G = 0$ profile this computation yields the solid curves given in Fig. 1, which are in good agreement with the data. The constant bump at position -4 mm is a systematic error due to an unfortunately placed wire inside the vacuum chamber that scatters the cloud fluorescence. This bump is therefore not suppressed by the background subtraction. We obtain the same experimental and theoretical cloud shapes when B_G is applied along $\hat{\mathbf{x}}$ instead of $\hat{\mathbf{y}}$. This is expected, as the $\pi/2$ rotation of B_G merely generates a quarter-wave shift of the grating pattern [δ in Eq. (1)].

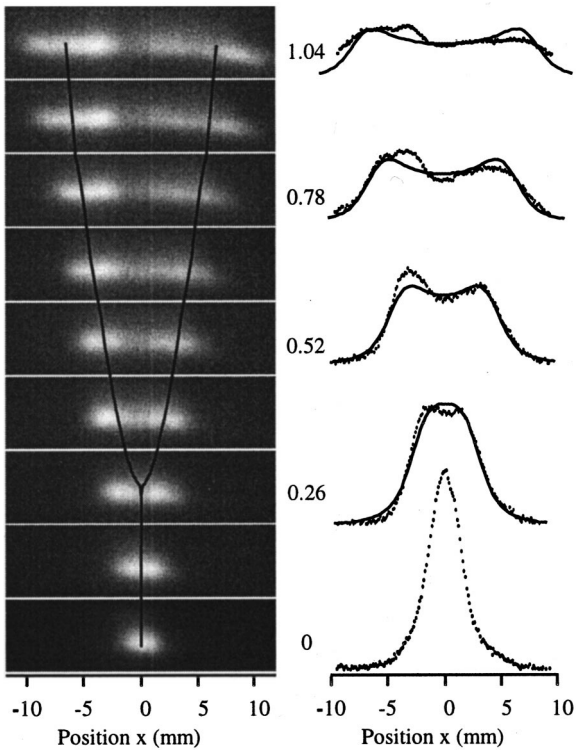

FIG. 1. Left: atom clouds split by bouncing on a corrugated concave reflector. Black lines show the positions of peaks predicted by our theory. Center: values of corrugating field B_G in gauss. Right: intensity profiles. Solid lines show theory; dots are experiment data. Normalization is the only fitting parameter.

This experiment demonstrates that a permanent-magnet reflector can be corrugated in a well-controlled way by an applied field, and it opens the way to real-time control of the reflecting surface. As a first demonstration of this we replaced the constant field by a modulated one $B_G \cos 2\pi f t\, \hat{\mathbf{y}}$. Figure 2 shows how the shape and width of the reflected cloud (FWHM) vary with f and B_G. At low frequency the grating is indistinguishable from a static one of amplitude B_G because the field is intentionally phased to reach its maximum when the center of the cloud reaches the grating (at 74 ms). At a few tens of Hz, the reflected cloud becomes narrower because there is a ± 5-ms thermal spread of the cloud and the early and late arrivals ''see'' less than the maximum corrugation. Above 100 Hz the ensemble averages over all oscillation phases, the profile becomes roughly triangular (inset in Fig. 2), and the width becomes constant. A second strong decrease in the width is seen below 15 kHz. This can be understood by recalling [Eq. (2)] that individual atoms spend a finite time $T_{\rm int} \approx 60\,\mu$s interacting with the mirror. When the oscillation period is shorter than $T_{\rm int}$, the transverse force averages away and the mirror becomes flat again. In the first run with an oscillating field, we noticed a strong resonant dip in the mirror reflectivity due to spin flips.

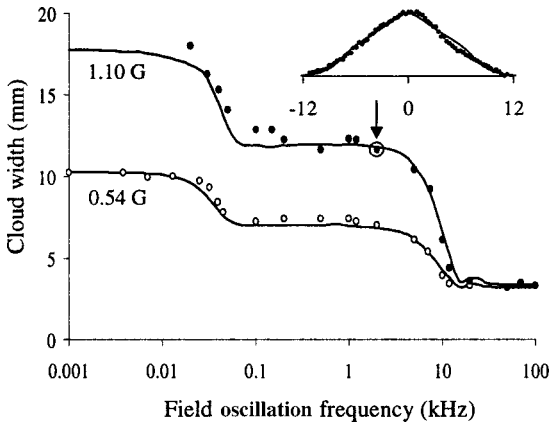

FIG. 2. Cloud widths after reflection from an oscillating grating. Experimental results are indicated by open and filled circles for applied fields of 0.54 and 1.10 G, respectively. Lines: calculated widths using numerical integration. Inset: cloud profile for a 2-kHz, 1.1-G grating with abscissa in millimeters.

This was moved to higher frequency by increasing B_z to 0.82 G, which gave unit reflectivity over the whole frequency range of Fig. 2. The two solid lines, calculated numerically from the equations of motion, show that we understand all the important physical effects. The agreement shows that, even though the applied field oscillates, it continues simply to add directly to the mirror field and μ_ζ remains an adiabatic constant.

In our final experiment we use a rotating field $B_G(\cos 2\pi ft\,\hat{\mathbf{x}} \pm \sin 2\pi ft\,\hat{\mathbf{y}})$ to corrugate the reflector. This causes the phase δ in Eq. (1) to grow as $\pm 2\pi ft$ and therefore makes a grating traveling along $\pm\hat{\mathbf{x}}$ [7]. Figure 3 shows how this grating influences the width and shape of the cloud. It no longer narrows at low frequency, because each atom ''sees'' a grating with the full depth B_G. Indeed, the profile inset into Fig. 3 shows that at 3 kHz, the cloud shape is the

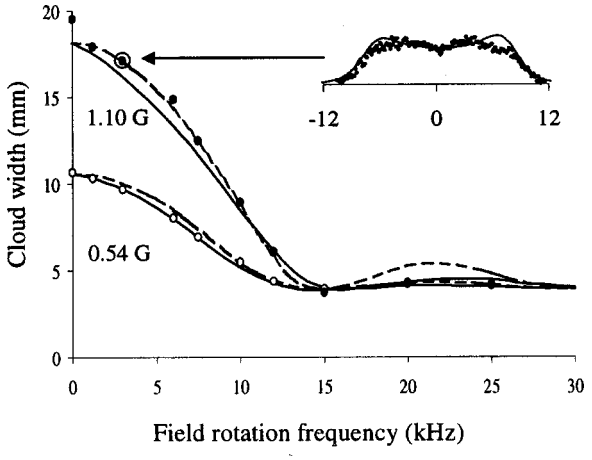

FIG. 3. Cloud widths after reflection from a traveling grating. Experimental results are indicated by open and filled circles for applied fields of 0.54 and 1.10 G, respectively. Solid lines: calculation using full equations of motion. Dashed lines: simplified theory described in the text. Inset: cloud profile for a 3-kHz, 1.1-G grating with abscissa in millimeters.

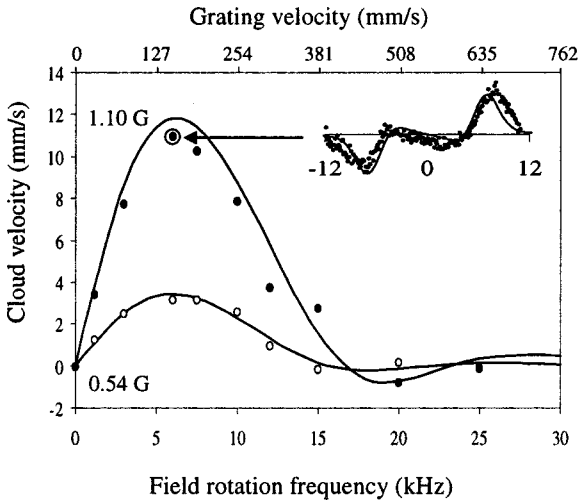

FIG. 4. Center-of-mass velocity transferred to the cloud from a traveling grating. Two abscissa show the frequency of the field and the corresponding grating velocity. Experimental results are indicated by open and filled circles for applied fields of 0.54 and 1.10 G, respectively. Lines: calculation using full equations of motion. Inset: difference between cloud profiles with left and right moving gratings at 6 kHz and 1.1 G.

same as that from a static grating, whereas the oscillating grating produced a triangular profile (as in Fig. 2). This is a clear demonstration that the grating is a purely traveling one with no appreciable standing component. Once again the mirror becomes flat for frequencies above 15 kHz. This frequency dependence can be derived assuming constant x, which gives the average horizontal force $\overline{F_x}$ on an atom incident at x as

$$\overline{F_x} = \frac{\sin(\pi f T_{\rm int})}{\pi f T_{\rm int}} k \mu_\zeta B_G \sin(kx + \pi f T_{\rm int}). \qquad (4)$$

The only difference between this and a static grating is the first factor, which amounts to a frequency-dependent roll-off of the effective static field strength. The dashed lines in Fig. 3 show the cloud widths resulting from this simple model, while the solid lines are the full time-dependent numerical theory. Both exhibit good agreement with the data. This roll-off is not fundamentally different from the recent observation by Henkel *et al.* [11] that scalar diffraction is suppressed at grazing incidence. To see this, we note that the velocity of the grating is $\mathbf{v}_{\rm grating} = f\lambda\hat{\mathbf{x}}$, while that of the incident atom is $-\sqrt{2gh}\,\hat{\mathbf{y}}$. In the frame of reference moving with the grating, grazing incidence therefore satisfies the condition $f\lambda > \sqrt{2gh}$, and from Eq. (2) one finds at once that this is essentially the same as the roll-off condition $fT_{\rm int} > 1$.

An exciting aspect of the traveling grating is that it offers the prospect of transporting cold atoms along a surface. In order to investigate the velocity transferred from the grating, we switched the propagation direction of the wave between $+\hat{\mathbf{x}}$ and $-\hat{\mathbf{x}}$ and measured the shift 2Δ in the center of mass of the cloud. Division of Δ by the 74-ms flight time gave the velocity $v_{\rm cloud}$, which we plot in Fig. 4. In this experiment, the atoms are not bound to the grating but pass transiently

through it. According to our calculations they are transported by less than a micron during $T_{\rm int}$. Nevertheless, we see that an appreciable center-of-mass velocity is still imparted to the cloud. This cannot be explained in the constant-x, Raman-Nath approximation, because that gives a symmetrical distribution of reflection angles; it is the ''surfing'' of the atoms on the moving grating that produces $v_{\rm cloud}$. We have calculated this numerically and find good agreement with the experiment (Fig. 4). At low frequency we find $v_{\rm cloud} \propto B_G^2 f$, with the usual roll-off bringing $v_{\rm cloud}$ back to zero at $f = 1/T_{\rm int}$. The graph inset into Fig. 4 shows the difference between cloud profiles for the two directions of a 6-kHz, 1.1-G grating. Naturally, the difference is most pronounced on the sides of the cloud near ± 8 mm.

Stronger coupling can be achieved between the atoms and the grating by increasing the strength of B_G. However, this also increases the width of the cloud, making it too wide to be imaged through our optical system. (It is already too large at 1.1 G dc—hence the absence of low-frequency points on the upper curve of Fig. 2). In order to move more closely towards the idea of an atom conveyor belt, the next step is to bind the atoms to the traveling wave, a project that is underway in our laboratory now.

In summary, we have demonstrated that a static magnetic mirror can be adapted by the addition of an external field to form a static, oscillating, or traveling grating of adjustable depth. The reflected clouds observed are in good agreement with theory and can be modulated at frequencies up to 15 kHz. We have also observed the momentum transferred to the center of mass of the cloud as a result of atoms surfing on the traveling wave.

We are indebted to Ben Sauer for much technical assistance. This work was supported by grants from EPSRC (UK), the British Council, the Royal Society, and the European Union.

[1] J. P. Dowling and J. Gea-Banacloche, Adv. At., Mol., Opt. Phys. **37**, 1 (1996); C. S. Adams and E. Riis, Prog. Quantum Electron. **21**, 1 (1997); V. Balykin, Adv. At., Mol., Opt. Phys. **41**, 181 (1999).

[2] E. A. Hinds and I. G. Hughes, J. Phys. D **32**, R119 (1999).

[3] T. M. Roach *et al.*, Phys. Rev. Lett. **75**, 629 (1995); I. G. Hughes *et al.*, J. Phys. B **30**, 647 (1997); **30**, 2119 (1997); C. V. Saba *et al.*, Phys. Rev. Lett. **82**, 468 (1999).

[4] A. I. Sidorov *et al.*, Quantum Semiclassic. Opt. **8**, 713 (1996); D. Meschede *et al.*, Proc. SPIE **2995**, 191 (1997).

[5] A. Steane *et al.*, Phys. Rev. Lett. **74**, 4972 (1995); P. Szriftgiser *et al.*, *ibid.* **77**, 4 (1996).

[6] K. S. Johnson *et al.*, Phys. Rev. Lett. **81**, 1137 (1998); D. C. Lau *et al.*, Eur. Phys. J. D **5**, 193 (1999).

[7] E. A. Hinds, Philos. Trans. R. Soc. London, Ser. A **357**, 1409 (1999).

[8] J. Schmiedmayer, Eur. Phys. J. D **4**, 57 (1998).

[9] J. H. Thywissen *et al.*, Eur. Phys. J. D **7**, 361 (1999); T. J. Davis, J. Opt. B: Quant. Semiclass. Opt. **1**, 408 (1999).

[10] G. I. Opat, S. J. Wark, and A. Cimmino, Appl. Phys. B: Photophys. Laser Chem. **54**, 396 (1992).

[11] C. Henkel, J. Y. Courtois, and A. Aspect, J. Phys. II **4**, 1955 (1994).